Fuzzy-AHP and AHP-Based Assessment of Seismic Hazard in Delhi-NCR Region, India

Abstract

The Delhi-National Capital Region (NCR) lies within Seismic Zones IV and V as per the Indian Earthquake Code IS:1893 (Part 1) - 2025, indicating a high level of seismic hazard. The region has experienced frequent small to moderate earthquakes in recent times. Additionally, high population density, rapid urbanisation, and many vulnerable structures increase the risk of human and economic loss during an earthquake, making this region more vulnerable. In the present study, a comparative seismic hazard assessment of the Delhi-NCR was conducted using geological data and multi-criteria decision-making methods, namely the Analytical Hierarchy Process (AHP) and Fuzzy-AHP. Findings indicate that 50% of the study region and about 45% of its population are in high seismic hazard zones, particularly in Panipat, Sonipat, and Rohtak. Seismic hazard across Delhi varies from low to very high, influenced by the nearby Himalayan collision zone and active faults such as the Delhi-Haridwar Ridge and Mahendragarh-Dehradun Fault. Ongoing convergence of the Indian and Eurasian plates generates tectonic stress capable of reactivating these faults. ROC analysis provided the accuracy values of 0.7880 for AHP and 0.7842 for Fuzzy-AHP, indicating that AHP performs marginally better, although the difference (0.0038) is minimal. The seismic hazard map developed through this analysis can help with urban planning, disaster preparedness, and the design of earthquake-resilient infrastructure.

Keywords: Seismic Hazard, Delhi-NCR, Analytical Hierarchy Process, Fuzzy-AHP, Spectral Acceleration, Receiver-Operator Characteristic (ROC)

1. Introduction

Earthquakes are among the most devastating natural hazards, often resulting in loss of life, widespread destruction of infrastructure, and significant socio-economic disruption at both national and regional levels (Duruel 2023; Polat, 2024). Globalisation, unplanned and rapid urbanisation, along with industrial growth have led to increased urban population density and the industrial zones, making them more vulnerable to seismic hazards (Çatkın and Toprak 2025). Consequently, the functional performance of urban environments in the aftermath of disasters is increasingly difficult to sustain. Addressing these challenges requires firsthand information about seismically hazardous zones, which provides a critical basis for integrating sustainable development objectives with resilient urban planning.

Over recent decades, rapid population growth in India has significantly reconfigured urban settlement patterns, with pronounced effects in metropolitan areas such as the Delhi--National Capital Region (NCR). Delhi's population has expanded to almost 19 million, driving accelerated urban sprawl and increased urban density (Kolathayar 2021). This growth has been facilitated by its strategic location and functional integration with surrounding cities, including Gurugram (Gurgaon), Faridabad, Sonipat, Noida, and Rohtak, establishing the region as a critical metropolitan hub. The Delhi-NCR has further consolidated its role as a major centre for commerce and education, intensifying pressures on the urban environment.

Urban development in the Delhi-NCR is critically challenged by its intraplate seismicity and proximity to major active Himalayan structures, notably the Main Boundary Thrust (MBT) and Main Central Thrust (MCT), which amplify the earthquake hazard (Seeber and Armbruster 1981). The Himalayan belt is a globally recognised hotspot of seismic activity, with a well-documented history of destructive earthquakes, such as the 2015 Gorkha, Nepal earthquake (Mw~7.8), which caused widespread damage and approximately 9,000 fatalities (Bilham 2019). More recently, the Mw~5.9 earthquake of 3rd October 2023, followed by a Mw~5.2 aftershock, generated strong ground shaking across western Nepal and northern India. Previous studies indicate that the region is overdue for one or more large-magnitude earthquakes comparable to the 2015 Gorkha event, highlighting the urgent need for seismic hazard mitigation in the Delhi-NCR (Bilham 2019).

The Delhi-NCR has a well-documented history of significant seismic activity, with numerous earthquakes exceeding a magnitude of 5.0 over several centuries. In recent years, seismic events on April 12, 2020, May 10, 2020, May 29, 2020, and October 15, 2023, have highlighted the regional seismic activity. Records from the National Centre for Seismology (NCS), India, reveal a concentration of seismic activity around Gurgaon (Gurugram), Rohtak, and Delhi. While the Delhi-NCR has not experienced a major earthquake in recent years, the region remains highly susceptible to seismic hazards. This risk is further amplified by extensive urbanisation, industrial expansion, and the area's socio-political significance, underscoring the critical importance of accurate seismic hazard mapping.

The implementation of Geographic Information Systems (GIS)-based Analytical Hierarchy Process (AHP) has been extensively used to understand the seismic hazard in different parts of the world (Karimzadeh et al. 2014; Abudeif et al. 2017; Wen et al. 2017; Al-Dogom et al. 2018; D'Alpaos and Valluzzi 2020; Fentahun et al. 2021; Flores et al. 2021; Moustafa et al. 2022; Ansari et al. 2025; Silahtar et al. 2025; Zakaria and Mahmoud 2025), whereas fuzzy-AHP has been applied only to a limited extent in seismic hazard assessment (Mokarram et al. 2021; Zheng et al. 2021; Yildirim et al. 2024). In India, several researchers have also utilised AHP to map seismic hazards in areas prone to earthquake events (Nath et al. 2015; Bhatt et al. 2019; Dwivedi et al. 2020; Pudi et al. 2021; Agrawal et al. 2022; Padder et al. 2022; Pancholi et al. 2022; Ellappa Subramani and Velapgy 2025). Fuzzy-AHP has been widely used in landslide, tsunami, flood, and other environmental hazard studies. However, its use for comprehensive seismic hazard assessment in India is still limited. In Delhi, Mohanty et al. (2007) employed AHP to develop a seismic microzonation map using Peak Ground Acceleration (PGA) contours, soil types at a depth of 6 m, geological conditions, groundwater fluctuations, and bedrock depth. The results indicated that a substantial portion of the Delhi region is exposed to high seismic hazard. Subsequently, Sinha et al. (2014) utilised a comprehensive spatial dataset comprising seismic zones, PGA, soil characteristics, liquefaction potential, geological features, land use, and proximity to faults and epicentres, to assess seismic hazard in the Delhi region, identifying the eastern part of the city as relatively more hazard-prone. More recently, Sahdev et al. (2020) applied an AHP-based framework to evaluate seismic vulnerability using parameters such as seismic microzonation, lineament density, bedrock depth, groundwater depth, built-up density, and population density, reporting that 5.40% of the study area falls within a very high seismic vulnerability zone. However, data availability remains a major challenge in seismic hazard mapping. Moreover, most existing studies are concentrated in the Delhi region and predominantly employ the AHP approach.

Addressing the gaps identified in the existing literature, this study conducts a comparative evaluation of AHP and Fuzzy-AHP models for seismic hazard mapping in the Delhi-NCR, India, using publicly available earthquake inventories and geological datasets. The findings aim to aid governmental authorities and disaster management agencies in developing more effective seismic hazard mitigation and preparedness strategies in this densely populated region.

2. Study Area

The Delhi-NCR area is situated within the Delhi-Aravalli Fold Belt, a major Precambrian tectonic domain extending across northern India and encompassing Delhi and adjoining areas of Rajasthan, Haryana and Uttar Pradesh (Fig. 1). This west–east trending belt is positioned between the Delhi-Haridwar Ridge and the Munger-Saharsa Ridge, with the Indo-Gangetic Plains to the north and the Aravalli Range to the south (Bansal et al., 2021). Due to its tectonic association with the Himalayan orogenic system, the region is considered highly prone to seismic activity (Kolathayar, 2021) and falls within seismic Zones IV and V as per IS-1893 Part 1 (2025). Earthquakes in this region are primarily driven by the ongoing collision between the Indian and Eurasian plates, a process that began during the early Cenozoic era. This collision gave rise to the Himalayan arc, inducing widespread crustal deformation within the arc and its foreland, and consequently increasing seismic hazards in the surrounding areas (Searle 1986).

The Delhi region, situated within the broader Himalayan seismic belt, is traversed by several major faults, including the Sohna, Mahendragarh-Dehradun, Mathura, Great Boundary and Moradabad faults, all of which are capable of generating seismic activity. According to Gahalaut and Kundu (2012), these structures represent reactivated basement faults that predate the collision between the Indian and Eurasian tectonic plates. Large parts of the region are mantled by thick sequences of older and younger alluvium, together with unconsolidated sediments of the Yamuna floodplain, which enhance susceptibility to ground-motion amplification during events (Srivastava 1988). The Delhi-NCR has experienced repeated damaging seismic events documented in both historical and instrumental records (Iyengar 2000). Notable earthquakes include an intensity IX event (M~6.5) near Sohna in 1720 (Oldham

1883), followed by moderate to strong earthquakes near Mathura in 1842 (M~5.0), near Bulandshahr in 1956 (M~6.7) (IMD, 2004) and near Sohna in 1960 (M~6.0) (Srivastava and Somayajulu 1966). In this century, from 2000 to 2023, the Delhi region recorded 128 seismic events of magnitude ≥ 3.0, with a maximum of 14 events in 2020. Hence, according to available data, this region is seismically vulnerable to a sufficient extent.

3. Data Source and Methodology

All the data incorporated in this study were collected from open-access sources. The details on the active fault were taken from Zelenin et al. (2022). The historical earthquake record for the study area, spanning 1966-2023, was obtained from the National Centre for Seismology (NCS), India. The starting period was selected to be 1966 as the 1960s marked the installation of the World-Wide Standardised Seismic Network, which supported the development and strengthening of national seismic monitoring systems in India. Peak ground acceleration (PGA) values were calculated using the ground-motion prediction equation developed by Caprio et al. (2015), which was selected for its consistency with globally established ground-motion-to-intensity conversion relationships. Lithological information was sourced from Universität Hamburg (Gleeson et al., 2011). Elevation data with a spatial resolution of 12.5 m were derived from ALOS PALSAR (ASF DAAC, 2014). Sediment thickness data were obtained from Pelletier et al. (2016), and the average shear-wave velocity to a depth of 30 m (V_{s30}) was retrieved from the USGS. The amplification factor has been derived from the empirical power-law relationship between Vs30 and the amplification factor. The spatial datasets were classified using the natural breaks method, and selected layers were resampled to a 12.5 m resolution to ensure spatial consistency across parameters. Numerous studies have demonstrated the influence of different thematic criteria on seismic hazard assessment outcomes (Jena et al. 2020; Yariyan et al. 2020). All the mentioned datasets were last accessed and verified in November 2025. The following section describes the methodology adopted for seismic hazard mapping in the Delhi–NCR region.

3.1. Multi-Criteria Decision-Making (MCDM) Models

MCDM methods provide a structured analytical framework that integrates expert judgment into complex decision problems (Zavadskas and Turskis 2011). These approaches systematically explore the problem complexity and enable the comparison and ranking of multiple alternatives based on carefully defined criteria (Malczewski and Liu 2014). In this study, the Analytical Hierarchy Process (AHP) and Fuzzy-AHP MCDM models were applied to map seismic hazard in the Delhi-NCR, and subsequently the results were compared to determine the suitability of an approach that provides a more robust assessment for the region (Fig. 2).

3.1.1. Analytical Hierarchy Process (AHP) and Fuzzy-Analytical Hierarchy Process (Fuzzy-AHP)

The AHP is a commonly used MCDM method that applies pairwise comparison matrices within a hierarchical framework to derive criterion weights (Saaty 1980). In this approach, importance values from 1 to 9 are assigned to each criterion based on their relative significance, typically assigned by expert opinion or existing studies (Table 1). In the present study, the comparison matrix was derived from the published literature published. The resulting comparison matrix is then normalised by dividing each entry by the sum of its respective column, and the final weights are obtained by calculating the average of each row in the normalised matrix.

The Fuzzy-AHP was developed to address hierarchical decision-making problems and overcome the key limitations of the AHP, particularly its reliance on precise scores from the decision-makers (Yaghoobi 2018). Although AHP is widely used as an MCDM approach, it is not sufficiently robust in handling the uncertainty inherent in data (Wątróbski et al. 2018). In contrast, Fuzzy-AHP effectively incorporates uncertainty through the principles of fuzzy set theory (Yariyan et al. 2020), enabling a more systematic approach to alternative selection (Buckley 1985; Chang 1996). This study has adopted Buckley's Fuzzy-AHP method due to its relative ease of calculation and its ability to produce a unique solution. In this approach, alternative weights are derived using a geometric mean formulation in combination with a trapezoidal membership function. Accordingly, a fuzzy pairwise comparison matrix $\tilde{D} = [\tilde{a}_{ij}]$ is constructed using a triangular fuzzy scale (Table 1), from which the fuzzy geometric mean value $\tilde{r}_i$, and weight $\tilde{w}_i$, are calculated as follows.

$$\tilde{r}_i = (\tilde{a}_{i1} * \tilde{a}_{i2} * \cdots * \tilde{a}_{in})^{1/n} \quad and \quad \tilde{w}_i = \tilde{r}_i * (\tilde{r}_1 + \tilde{r}_2 \cdots + \tilde{r}_n)^{-1} \tag{1}$$

The resulting fuzzy weights were subsequently defuzzified using the Centre-of-Area (COA) method using the following expression:

$$\widetilde{w_i} = \frac{l_i + m_i + u_i}{3} \quad (2)$$

The consistency of the judgments is then assessed using the Consistency Ratio (CR) in both the AHP and the Fuzzy-AHP models, as defined by the following equation.

$$CI = \frac{(\lambda_{max} - n)}{(n - 1)} \text{ and } CR = \frac{CI}{RI} \quad (3)$$

where λ_{max} is the principal eigenvalue, *n* the number of criteria employed, and RI the associated randomness index (Table 2). For fuzzy-AHP, to assess consistency, the pairwise comparison matrix was converted into crisp values using the centre-of-area method. When the CR value is below 0.1, the judgments are considered reliably consistent, allowing for a reliable evaluation of criterion priorities.

4. Results and Discussions

The AHP and Fuzzy-AHP comparison matrix is tabulated in Table 3, along with the corresponding weights for each parameter. The analysis of this study indicates that the western and a portion of the southern parts of Delhi-NCR are located in a highly seismically hazardous zone. This includes the districts Panipat, Sonipat, Rohtak, Rewari and Alwar. Delhi spans zones ranging from low to very high seismic hazard. The western and southern parts are predominantly categorised as high-hazard areas, whereas the eastern part mainly falls within low to moderate hazard levels (Fig. 3). The numerical values show that both models yield closely aligned results. According to the AHP model, 49.57% of the region is classified as high to very high hazard, 25.01% as moderate, 17.70% as low, and 8.25% as very low hazard. In terms of population distribution, 44.43% of residents live in high to very high hazard zones, 34.02% in moderate zones, 15.93% in low hazard areas, and 5.62% in very low hazard areas. Similarly, the fuzzy-AHP approach shows that 49.98% of the area falls within the high to very high hazard category, 27.63% is moderate, 15.55% is low, and 6.84% is classified as very low hazard. The study area has 45.14% of its inhabitants residing in a highly seismically hazardous zone, 36.46% in a moderate zone, 13.94% in a low zone, and 4.46% in a very low zone (Table 4).

The pronounced seismic hazard in the Delhi-NCR may be attributed to high active fault density, historical seismicity, and complex geological features, which collectively enhance earthquake susceptibility. The Delhi-NCR has experienced both near- and far-field earthquakes, reflecting its exposure to local and distant seismic sources due to its proximity to the Himalayan arc and regional tectonics (Abhishek et al. 2024). Several devastating Himalayan earthquakes, including the recent 2015 Gorkha earthquake (Mw~7.8) and 2023 Nepal earthquake (Mw~5.9), were felt in Delhi and its vicinity. The regional tectonics indicate that over 150 earthquakes with a magnitude (M) of 3.0 or greater have occurred in the study area from 1966 to 2023, according to the available dataset, which includes the March 2012 Bahadurgarh (Haryana-Delhi border) earthquake with a magnitude of ~5.10 and a maximum intensity of VI. Its epicentre was 4 km west of the Mahendragarh Dehradun Fault. This earthquake, classified as a non-Himalayan event, produced maximum intensity in the Jhajjar and Rohtak districts (Gupta et al. 2013), resulting in casualties, injuries, and extensive structural damage. Seismic records indicate that between 2001 and 2004, nearly 19 earthquakes with magnitudes above Mw 3.0 occurred within Delhi and the Delhi Fold Belt. Subsequent events on 29 May 2011 (Mw~3.4) and 1 June 2017 (M_w~4.2) occurred to the west of the Mahendragarh-Dehradun Fault (MDF), at approximate distances of 18 km and 7 km, respectively. In 2020, three earthquakes (Mw ~3.5, ~3.4, and ~4.5) impacted Delhi and its adjacent regions on 12 April, 10 May, and 29 May. The first two events occurred along the eastern borders of the Delhi-NCR, whereas the 29 May earthquake occurred near Rohtak, in proximity to the MDF. Earthquake records from the past five decades show that seismicity in the NCR is primarily clustered along major fault systems, particularly the MDF and the Sohna Fault (Dhali et al. 2023). Increased seismicity has been recorded along the western and southern borders of Delhi, primarily linked to the MDF and the Great Boundary Fault, while subsidiary structures, including the north-south-trending Sohna Fault, further modulate the spatial distribution of earthquakes in the region (Sandhu et al. 2022).

As discussed earlier, this region falls under Seismic Zones V and IV, corresponding to peak ground acceleration of 0.50 g and 0.75 g, for a return period of 2475 years (IS-1893 Part 1, 2025). Previous studies also show wide variability in estimated peak ground acceleration (PGA) for the Delhi-NCR region. Sandhu et al. (2020) reported PGA values of 0.10-0.60 g, with higher values at Sonipat, Gurugram and Faridabad, whereas strong-motion analysis by Pandey et al. (2020) indicated a much lower maximum PGA of 0.014 g near Delhi. Probabilistic assessments by Sreejaya et al. (2022) further reported PGA values ranging from 0.05g to 0.76 g for different return periods, highlighting the strong dependence of PGA estimates on hazard level. Recent work by Kumar et al. (2024) indicates that spectral acceleration (S_a) across the Delhi–NCR region reaches its maximum at short periods (T = 0.2 s) for return periods of 475 and 2475 years, with values spanning 0.60-1.18 g, whereas longer-period motion (T = 1.0 s) is characterized by lower S_a levels of 0.12–0.27 g. A comparable pattern is observed in the Gurgaon (Gurugram) area, where S_a at 0.2 s ranges from 0.61 to 1.19 g and decreases to 0.13-0.28 g at 1.0 s. Relatively high S_a values are also reported for Rohtak (0.43-0.70 g), Faridabad (0.48-0.97 g) and Noida (0.46-0.95 g), while Baraut (0.20-0.34 g), Sonipat (0.32-0.60 g) and Rewari (0.39-0.82 g) exhibit comparatively lower seismicity for the same hazard levels. These results reveal pronounced spatial heterogeneity in seismic response within the Delhi–NCR region.

Geological studies categorise the Delhi-NCR region into two distinct lithological units. The first comprises ancient quartz-bearing rocks that form a ridge in the south-central sector of the capital, Delhi. The second unit consists of alluvial deposits, whose thickness ranges from approximately 40 ft to over 980 ft across the Delhi-NCR. These alluvial sediments are primarily derived from rivers draining the Himalayas, with the Yamuna River contributing unconsolidated material along the eastern corridor (Sharma et al. 2015). Seismic waves propagating through such alluvial deposits experience reduced velocity and often increased amplitude, amplifying ground shaking and potentially inducing soil liquefaction or structural failure (Sharma et al. 2015). Shallow alluvium is particularly susceptible to liquefaction, while deeper deposits remain relatively stable. In floodplain zones, unconsolidated sediments can markedly intensify seismic effects. Therefore, design strategies need to explicitly incorporate measures to mitigate the life risk, especially when planning multistoried structures.

With rapid, unplanned urbanisation and population growth in the Delhi-NCR, the region has emerged as a critical driver of increasing stress on resources, including groundwater. Tiwari et al. (2021) proposed that non-tectonic forces, whether caused by natural processes or human activities, can affect seismic activity rates in both plate-boundary zones and tectonically stable continental interiors. According to their findings, seismic activity within the Aravalli-Delhi Fold Belt may be affected by human-induced groundwater extraction, which can destabilise faults through non-tectonic processes, as well as by seasonal hydrological unloading of the alluvial aquifer. Nonetheless, the primary faulting mechanism remains controlled by tectonic forces.

4.1. Validation of the models

Receiver Operating Characteristic (ROC) analysis was employed to validate and compare the performance of the proposed seismic hazard models for Delhi-NCR. Since ROC analysis relies on probabilistic inputs to assess binary classification performance, the seismic hazard map was converted into probability values (Fawcett 2006). Model performance was quantified using the Area Under the Curve (AUC), with the diagonal line representing a random classifier as a baseline. The AHP model achieved an AUC of 0.7880, corresponding to an accuracy of 78.80% (Fig. 4), whereas the Fuzzy-AHP model yielded an AUC of 0.7842 (78.42%). These results indicate that the AHP-based approach marginally outperforms the Fuzzy-AHP model in seismic hazard prediction. The reason is attributed to the fact that the weights are derived from established literature rather than subjective expert judgments, which may result in low uncertainty, as the added fuzzification may not significantly improve outcomes. However, Fuzzy-AHP is more advantageous mainly when vagueness and linguistic ambiguity dominate expert evaluations (Buckley, 1985; Chang, 1996). Nevertheless, further improvements in hazard assessment can be achieved by incorporating higher-resolution datasets. Potential limitations of the adopted framework include computational complexity, data inconsistencies, challenges in assigning criterion weights, and scalability issues, that should draw the path for future research.

5. Conclusions

Geospatial technologies have significantly advanced the assessment of disaster-prone zones, including seismic hazard, by enabling the acquisition, analysis, and visualisation of high-resolution spatial data. These tools enhance the characterisation of seismic hazards and inform evidence-based decision-making for earthquake hazard management and disaster mitigation. In this paper, a comparative study was conducted in which AHP and Fuzzy-AHP MCDM frameworks were applied to evaluate seismic hazard in the Delhi-NCR. Situated in Seismic Zones IV and V, Delhi-NCR faces high earthquake risk due to Himalayan tectonics. The region is intersected by several major faults, including the Sohna, Mahendragarh–Dehradun, Mathura, Great Boundary, and Moradabad faults, which, together with ongoing Himalayan seismic activity, contribute to the study area's overall seismic hazard.

Regarding hazardous areas, both models show a similar pattern, with the western and southern parts of the Delhi-NCR located in a highly seismically hazardous zone, which includes the districts of Panipat, Sonipat, Rohtak, Rewari and Alwar. Delhi remains in the shadow of multiple seismic hazard zones: the west and south are largely in high-hazard areas, while the east falls in low to moderate hazard zones. The numerical value also shows a similar result in which the AHP model indicates that 49.57% of the study area and 44.43% of its total inhabitants reside in the highly seismic hazard zone. The application of the fuzzy-AHP indicates that 49.98% of the study area and 45.14% of its inhabitants residing in a highly seismically hazardous zone. Validation through the ROC curve on the basis of AUC estimates, it is observed that the AHP-based approach marginally outperforms the Fuzzy-AHP model in seismic hazard prediction in the study area due to a strong data-centric support rather than relying on subjective expert judgment, thereby reducing uncertainty and limiting the added benefit from fuzzification. The findings from this study can primarily aid planning and disaster mitigation organisations in identifying earthquake-prone areas, managing land-use planning, risk-reduction initiatives, and enhancing preparedness for seismic events.

Declaration

Funding

The research was not supported by any funding.

References

Abhishek, Sandhu, M., Sharma, B.: Source characteristics of earthquakes in Delhi and its vicinity: Implications for seismogenesis in the stable continental region of India. Nat. Hazard. Res. 4, 448-458 (2024). https://doi.org/10.1016/j.nhres.2023.11.003

Abudeif, A.M., Abdelmoneim, A.A., Farrag, A.F.: GIS-based multi-criteria earthquake hazards evaluation using analytic hierarchy process for a nuclear power plant site, west Alexandria, Egypt. Environ. Earth Sci. 76, 796 (2017). https://doi.org/10.1007/s12665-017-7148-x

Agrawal, N., Gupta, L., Dixit, J., Dash, S. K.: Seismic risk assessment for the North Eastern Region of India by integrating seismic hazard and social vulnerability. Sustainable Resilient Infrastruct. 8(sup1), 102-132 (2023). https://doi.org/10.1080/23789689.2022.2133764

Al-Dogom, D., Schuckma, K., Al-Ruzouq, R.: Geostatistical seismic analysis and hazard assessment; United Arab Emirates. Int. Arch. Photogramm. Remote Sens. Spatial Inf. Sci. XLII-3/W4, 29-36, https://doi.org/10.5194/isprs-archives-XLII-3-W4-29-2018, 2018.

Ansari, A., El-Hussain, I., Deif, A. et al.: Integrated GIS-AHP based assessment of earthquake vulnerability and risk for urban residential buildings in Muscat, Sultanate of Oman. Sci. Rep. 15, 31995 (2025). https://doi.org/10.1038/s41598-025-17618-6

ASF DAAC.: ALOS PALSAR High Resolution Radiometric Terrain Corrected Product [Data set]. NASA Alaska Satellite Facility Distributed Active Archive Center (2014). https://doi.org/10.5067/Z97HFCNKR6VA

Bansal, B.K., Mohan, K., Verma, M. et al.: A holistic seismotectonic model of Delhi region. Sci, Rep. 11, 13818 (2021). https://doi.org/10.1038/s41598-021-93291-9

Bhatt, N., Pancholi, V., Chopra, S. et al.: Rapid seismic hazard assessment of the Sabarmati River basin in Gujarat State, Western India using GIS techniques. Bull. Eng. Geol. Environ. 78, 3927-3942 (2019). https://doi.org/10.1007/s10064-018-1373-8

Bilham, R.: Himalayan earthquakes: a review of historical seismicity and early 21st century slip potential. Geol. Soc. London 483(1), 423-482 (2019). https://doi.org/10.1144/SP483.16

BIS.: IS 1893 (Part 1): Indian Standard Criteria for Earthquake Resistant Design of Structures - General Provisions and Buildings, (Seventh Revision) (2025).

Buckley, J.J.: Fuzzy hierarchical analysis. Fuzzy Sets Syst, 17, 233-247 (1985). https://doi.org/10.1016/0165-0114(85)90090-9

Caprio, M., Tarigan, B., Worden, B.C., Wiemer, S., Wald, D.J.: Ground motion to intensity conversion equations (GMICEs): A global relationship and evaluation of regional dependency. Bull. Seismol. Soc. Am. 105, 1476-1490 (2015). https://doi.org/10.1785/0120140286

Çatkın, Ş., Toprak, A.: Integrated seismic risk assessment using multi-criteria decision making, statistical, and machine learning approaches: a case study of Denizli, Türkiye. Nat. Hazards 121, 21995-22025 (2025). https://doi.org/10.1007/s11069-025-07674-6

Chang, D.Y.: Applications of the extent analysis method on fuzzy AHP. Eur. J. Oper. Res. 95, 649-655 (1996). https://doi.org/10.1016/0377-2217(95)00300-2

D'Alpaos, C., Valluzzi, M.R.: Protection of Cultural Heritage Buildings and Artistic Assets from Seismic Hazard: A Hierarchical Approach. Sustainability, 12(4), 1608 (2020). https://doi.org/10.3390/su12041608

Dhali, M., Gadhavi, M.S., Mohan, K., et al.: Active faults studies in Delhi and national capital region (NCR): Inferences from satellite data and field investigations. Front. Earth Sci. 11, 1092927 (2023). https://doi.org/10.3389/feart.2023.1092927

Duruel, M.: The role of non-governmental organizations in disaster management: the case of hatay, 6 February earthquake. Uluslararası Politik Arastırmalar Dergisi 9(2), 1-17 (2023). https://doi.org/10.25272/icps.1332511

Dwivedi, V.K., Dubey, R.K., Pancholi, V. et al.: Multi criteria study for seismic hazard assessment of UNESCO world heritage Ahmedabad City, Gujarat, Western India. Bull. Eng. Geol. Environ. 79, 1721-1733 (2020). https://doi.org/10.1007/s10064-019-01644-6

Ellappa Subramani, S., Velapgy, M.M.: Evaluation of geo-factor weights with ESWA and AHP techniques for GIS-based seismic hazard modeling of Thiruvananthapuram city. Arab. J. Geosci. 18, 176 (2025). https://doi.org/10.1007/s12517-025-12321-2

Fawcett, T.: An introduction to ROC analysis. Pattern Recogn Lett. 27(8), 861-874 (2006). https://doi.org/10.1016/j.patrec.2005.10.010

Fentahun, T.M., Bagyaraj, M., Melesse, M.A., Korme, T.: Seismic hazard sensitivity assessment in the Ethiopian Rift, using an integrated approach of AHP and DInSAR methods. Egyptian J. Remote Sensing Space Science 24(3), 735-744 (2021). https://doi.org/10.1016/j.ejrs.2021.05.001

Flores, K.L., Escudero, C.R., Zamora-Camacho, A.: Multicriteria seismic hazard assessment in Puerto Vallarta metropolitan area, Mexico. Nat. Hazards 105, 253-275 (2021). https://doi.org/10.1007/s11069-020-04308-x

Gahalaut, V., Kundu, B.: Possible influence of subducting ridges on the Himalayan arc and on the ruptures of great and major Himalayan earthquakes. Gond. Res. 21(4), 1080-1088 (2012). https://doi.org/10.1016/j.gr.2011.07.021

Gleeson, T., Smith, L., Moosdorf, N., et al.: Mapping permeability over the surface of the earth. Geophys. Res. Lett. 38 (2011). https://doi.org/10.1029/2010GL045565

Gupta, S., Mohanty, W.K., Prakash, R., Shukla, A.K.: Crustal heterogeneity and seismotectonics of the national capital region, Delhi, India. Pure Appl. Geophys. 170 (4), 607-616 (2013). https://doi.org/10.1007/s00024-012-0572-7

IMD, 2004. Report on Micro Earthquake Survey of the Jind Region (Haryana) (2004), pp. 1-8

Iyengar, R.: Seismic status of Delhi megacity. Curr. Sci. 78(5), 568-574 (2000).

Jena, R., Pradhan, B., Beydoun, G., et al.: Earthquake hazard and risk assessment using machine learning approaches at Palu, Indonesia. Sci. Total Environ. 749, 141582 (2020). https://doi.org/10.1016/j.scitotenv.2020.141582

Karimzadeh, S., Miyajima, M., Hassanzadeh, R., et al.: A GIS-based seismic hazard, building vulnerability and human loss assessment for the earthquake scenario in Tabriz. Soil Dyn. Earthquake Eng. 66, 263-280 (2014). https://doi.org/10.1016/j.soildyn.2014.06.026

Kolathayar S., Sitharam T., Vipin K.: Deterministic seismic hazard macrozonation of India. J. Earth Syst. Sci. 121, 1351-1364 (2012). https://doi.org/10.1007/s12040-012-0227-1

Kolathayar, S.: Recent seismicity in Delhi and population exposure to seismic hazard. Nat. Hazards 109, 2621-2648 (2021). https://doi.org/10.1007/s11069-021-04936-x

Kannan, D., Khodaverdi, R., Olfat, L.: Integrated fuzzy multi-criteria decision-making method and multiobjective programming approach for supplier selection and order allocation in a green supply chain. J. Clean. Prod. 47, 355-367 (2013). https://doi.org/10.1016/j.jclepro.2013.02.010

Kumar, R., Yadav, R.B.S., Mittal, H. et al.: Probabilistic seismic hazard assessment of Delhi (National Capital Region) and its adjoining region, India. Environ. Earth Sci. 83, 586 (2024). https://doi.org/10.1007/s12665-024-11895-6

Malczewski, J., Liu, X.: Local ordered weighted averaging in GIS-based multi-criteria analysis. Ann. GIS 20(2), 117-129 (2014). https://doi.org/10.1080/19475683.2014.904439

Mohanty, W.K., Walling, M.Y., Nath, S.K. et al.: First Order Seismic Microzonation of Delhi, India Using Geographic Information System (GIS). Nat. Hazards 40, 245-260 (2007). https://doi.org/10.1007/s11069-006-0011-0

Mokarram, M., Negahban, S., Abdeldjalil, B.: GIS-based fuzzy-analytic network process (FAHP), fuzzy-analytic hierarchy process (FANP) methods and feature selection algorithm (FSA) to determine earthquake-prone areas in Kermanshah Province. Environ. Earth Sci. 80, 633 (2021). https://doi.org/10.1007/s12665-021-09934-7

Moustafa, S.S.R., Abdalzaher, M.S., Naeem, M., Fouda, M.M.: Seismic Hazard and site suitability evaluation based on multicriteria decision analysis. IEEE Access 10, 69511-69530 (2022). https://doi.org/10.1109/ACCESS.2022.3186937

Nath, S.K., Adhikari, M.D., Devaraj, N., Maiti, S. K.: Seismic vulnerability and risk assessment of Kolkata City, India, Nat. Hazards Earth Syst. Sci. 15, 1103-1121, https://doi.org/10.5194/nhess-15-1103-2015, 2015

Oldham, T.A.: Catalogue of Indian earthquakes. Mem. Geol. Surv. India 19, 163-215 (1883).

Padder, A.H., Nandy, S., Kothyari, G.C. et al.: Geomorphometric Appraisal for Seismic Hazard Assessment in the Chenab River Basin of the NW Himalayas, India. Geotecton. 56, 534-563 (2022). https://doi.org/10.1134/S0016852122040069

Pancholi, V., Bhatt, N., Singh, P. et al.: Multi-criteria approach using GIS for macro-level seismic hazard assessment of Kachchh Rift Basin, Gujarat, western India-First step towards earthquake disaster mitigation. J. Earth Syst. Sci. 131, 3 (2022). https://doi.org/10.1007/s12040-021-01744-6

Pandey, A.P., Suresh, G., Singh, A.: A widely felt Tremor (ML 3.5) of 12 April 2020 in and around NCT Delhi in the backdrop of prevailing COVID-19 pandemic lockdown: analysis and observations. Geomat. Nat. Hazards Risk 11(1), 1638-1652 (2020). https://doi.org/10.1080/19475705.2020.1810785

Pelletier, J.D., Broxton, P.D., Hazenberg, P.: Global 1-km Gridded Thickness of Soil, Regolith, and Sedimentary Deposit Layers. ORNL DAAC, Oak Ridge, Tennessee, USA (2016). http://dx.doi.org/10.3334/ORNLDAAC/1304

Polat, O.: The importance and necessity of psychological first aid competency through the observations and experiences of volunteer librarians in the earthquake zone. Bilgi Dunyasi 25(1), 118-149 (2024). https://doi.org/10.15612/BD.2024.745

Pudi, R., Martha, T.R., Roy, P. et al.: Mesoscale seismic hazard zonation in the Central Seismic Gap of the Himalaya by GIS-based analysis of ground motion, site and earthquake-induced effects. Environ. Earth Sci. 80, 613 (2021). https://doi.org/10.1007/s12665-021-09907-w

Saaty, T.L.: The analytic hierarchy process: Planning, priority setting, resource allocation. New York: McGraw 281 (1980).

Sahdev, S., Kumar, M., Singh, R.B.: Seismic vulnerability assessment of NCT of Delhi using GIS-based multiple criteria decision analysis. Sahdev, S., Singh, R., Kumar, M. (eds).

Geoecology of Landscape Dynamics. Advances in Geographical and Environmental Sciences, Springer, Singapore (2020). https://doi.org/10.1007/978-981-15-2097-6_2

Sandhu, M., Sharma, B., Mittal, H.: Simulation of strong ground motion due to active Sohna fault in Delhi, National Capital Region (NCR) of India: an implication for imminent plausible seismic hazard. Nat. Hazards 104, 2389–2408 (2020). https://doi.org/10.1007/s11069-020-04277-1

Sandhu, M., Yadav, R.B.S., Kumar, R.: Spatial variability of earthquake hazard parameters, return periods and probabilities of earthquake occurrences in the eastern Himalayan seismic belt. Phys. Chem. Earth 127, 103194 (2022). https://doi.org/10.1016/j.pce.2022.103194

Searle, M.P.: Structural evolution and sequence of thrusting in the High Himalayan, Tibetan-Tethys and Indus suture zones of Zanskar and Ladakh, Western Himalaya. J. Struct. Geol. 8(8), 923-936 (1986). https://doi.org/10.1016/0191-8141(86)90037-4

Seeber, L., Armbruster, J.G.: Great detachment earthquakes along the Himalayan arc and long-term forecasting. Simpson DW, Richards PG (eds). Earthquake prediction-an international review: maurice ewing series. Am. Geophy. Uni. 4, 259-277 (1981).

Sharma, B., Chingtham, P., Sutar, A.K., Chopra, S., Shukla, H.P.: Frequency dependent attenuation of seismic waves for Delhi and surrounding area, India. Ann. Geophys. 58(2) (2015). https://doi.org/10.4401/ag-6636

Silahtar, A., Karaaslan, H., Kocaman, K., Senkaya, M., Albayrak, F.: Multi-criteria microzonation Hazard assessment based on the analytic hierarchy process framework. Geomatics Nat. Hazards Risk 16(1) (2025). https://doi.org/10.1080/19475705.2025.2584701

Sinha, N., Priyanka, N., Joshi, P. K.: Using Spatial Multi-Criteria Analysis and Ranking Tool (SMART) in earthquake risk assessment: a case study of Delhi region, India. Geomatics Nat. Hazards Risk 7(2), 680-701 (2016). https://doi.org/10.1080/19475705.2014.945100

Sreejaya, K., Raghukanth, S., Gupta, I.: Seismic hazard map of India and neighbouring regions. Soil Dyn. Earthq. Engg. 163, 107505 (2022). https://doi.org/10.1016/j.soildyn.2022.107505

Srivastava, L.S., Somayajulu J.G.: The seismicity of area around Delhi. Proc. III Symposium on Earthquake Engg, Univ. of Roorkee, 417-422 (1966).

Srivastava, A.: Geoscientific appraisal of Najafgarh depression and related environmental problems of Delhi. Geomorp. Environ., 631-642 (1988).

Tiwari, D.K., Jha, B., Kundu, B. et al. Groundwater extraction-induced seismicity around Delhi region, India. Sci Rep 11, 10097 (2021). https://doi.org/10.1038/s41598-021-89527-3

Wątróbski, J., Jankowski, J., Ziemba P.: Generalised framework for multi-criteria method selection. Omega 86, 107-124 (2018). https://doi.org/10.1016/j.omega.2018.07.004

Wen, H., Xie, P., Xiao, P. et al.: Rapid susceptibility mapping of earthquake-triggered slope geohazards in Lushan County by combining remote sensing with the AHP model developed for the Wenchuan earthquake. Bull. Eng. Geol. Environ. 76, 909-921 (2017). https://doi.org/10.1007/s10064-016-0957-4

Yaghoobi, T.: Prioritising key success factors of software projects using fuzzy AHP. J. Softw: Evol. Process 30(1), 1891 (2018). https://doi.org/10.1002/smr.1891

Yariyan, P., Zabihi, H., Wolf, I.D.: Earthquake risk assessment using an integrated Fuzzy Analytic Hierarchy Process with Artificial Neural Networks based on GIS: A case study of Sanandaj in Iran. Int. J. Disaster Risk Reduct. 50, 101705 (2020). https://doi.org/10.1016/j.ijdrr.2020.101705

Yildirim, A.K., Kavus, B.Y., Karaca, T.K. et al.: A novel seismic vulnerability assessment for the urban roadway by using interval valued fermatean fuzzy analytical hierarchy process. Nat. Hazards 120, 13811-13834 (2024). https://doi.org/10.1007/s11069-024-06748-1

Zakaria, G., Mahmoud, B.: Comprehensive Seismic Vulnerability Assessment of Tunnels: Application of the Analytic Hierarchy Process (AHP) in Algeria. Indian Geotech. J. (2025). https://doi.org/10.1007/s40098-025-01434-w

Zavadskas, E.K., Turskis, Z.: Multiple criteria decision making (MCDM) methods in economics: An overview. Technol. Econ. Dev. Econ. 17, 397-427 (2011). https://doi.org/10.3846/20294913.2011.593291

Zelenin, E., Bachmanov, D., Garipova, S., Trifonov, V., Kozhurin, A.: The Active Faults of Eurasia Database (AFEAD): the ontology and design behind the continental-scale dataset. Earth Syst. Sci. Data 14, 4489-4503 (2022). https://doi.org/10.5194/essd-14-4489-2022.

Zheng, Q., Lyu, H.M., Zhou, A., Shen, S.L.: Risk assessment of geohazards along Cheng-Kun railway using fuzzy AHP incorporated into GIS. Geomatics Nat. Hazards Risk 12(1), 1508-1531 (2021). https://doi.org/10.1080/19475705.2021.1933614

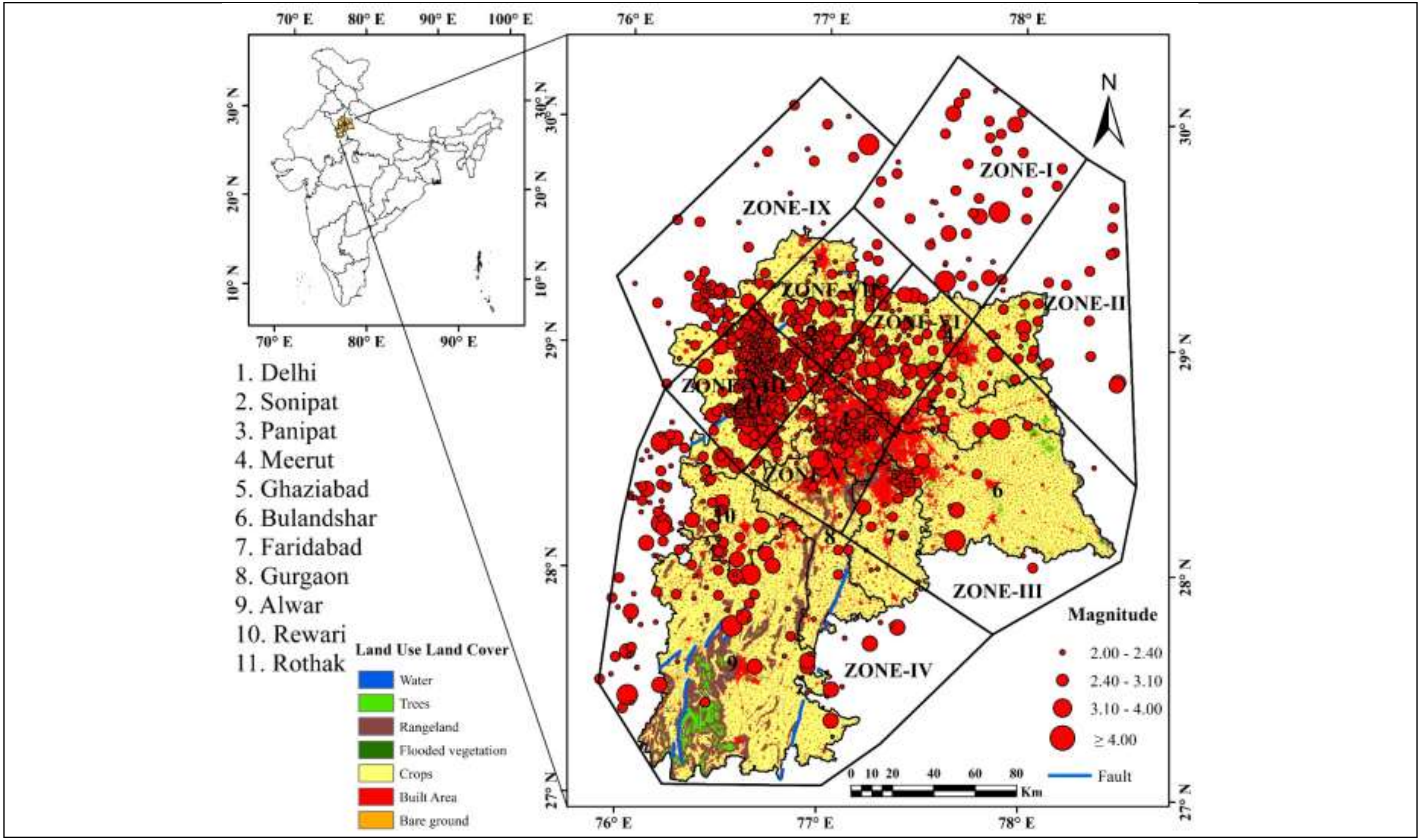

70° E
80° E
90° E
100° E
70° E
80° E
90° E
30° N
20° N
10° N
76° E
77° E
78° E
30° N
29° N
28° N
27° N
N
ZONE-I
ZONE-II
ZONE-III
ZONE-IV
ZONE-V
ZONE-VI
ZONE-VII
ZONE-VIII
ZONE-IX
1. Delhi
2. Sonipat
3. Panipat
4. Meerut
5. Ghaziabad
6. Bulandshar
7. Faridabad
8. Gurgaon
9. Alwar
10. Rewari
11. Rothak
Land Use Land Cover
Water
Trees
Rangeland
Flooded vegetation
Crops
Built Area
Bare ground
Magnitude
2.00 - 2.40
2.40 - 3.10
3.10 - 4.00
≥ 4.00
Fault
0 10 20 40 60 80
Km

Figure 1: Location of the study area. The active faults, earthquake locations (1956-2025) and land use and land cover information (Sentinel 2) have been provided for reference.

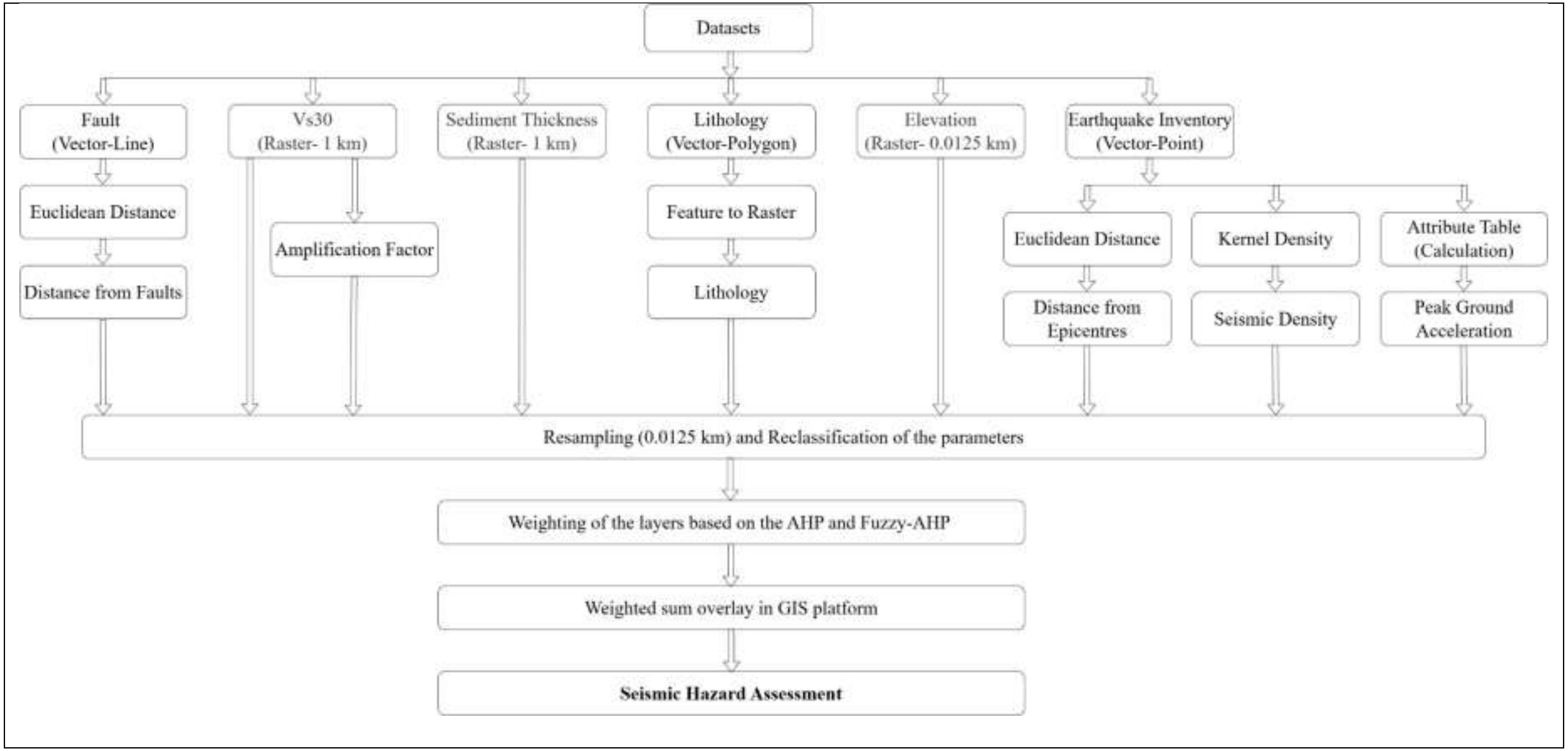

Figure 2: Flowchart illustrating the methodology adopted in this analysis.

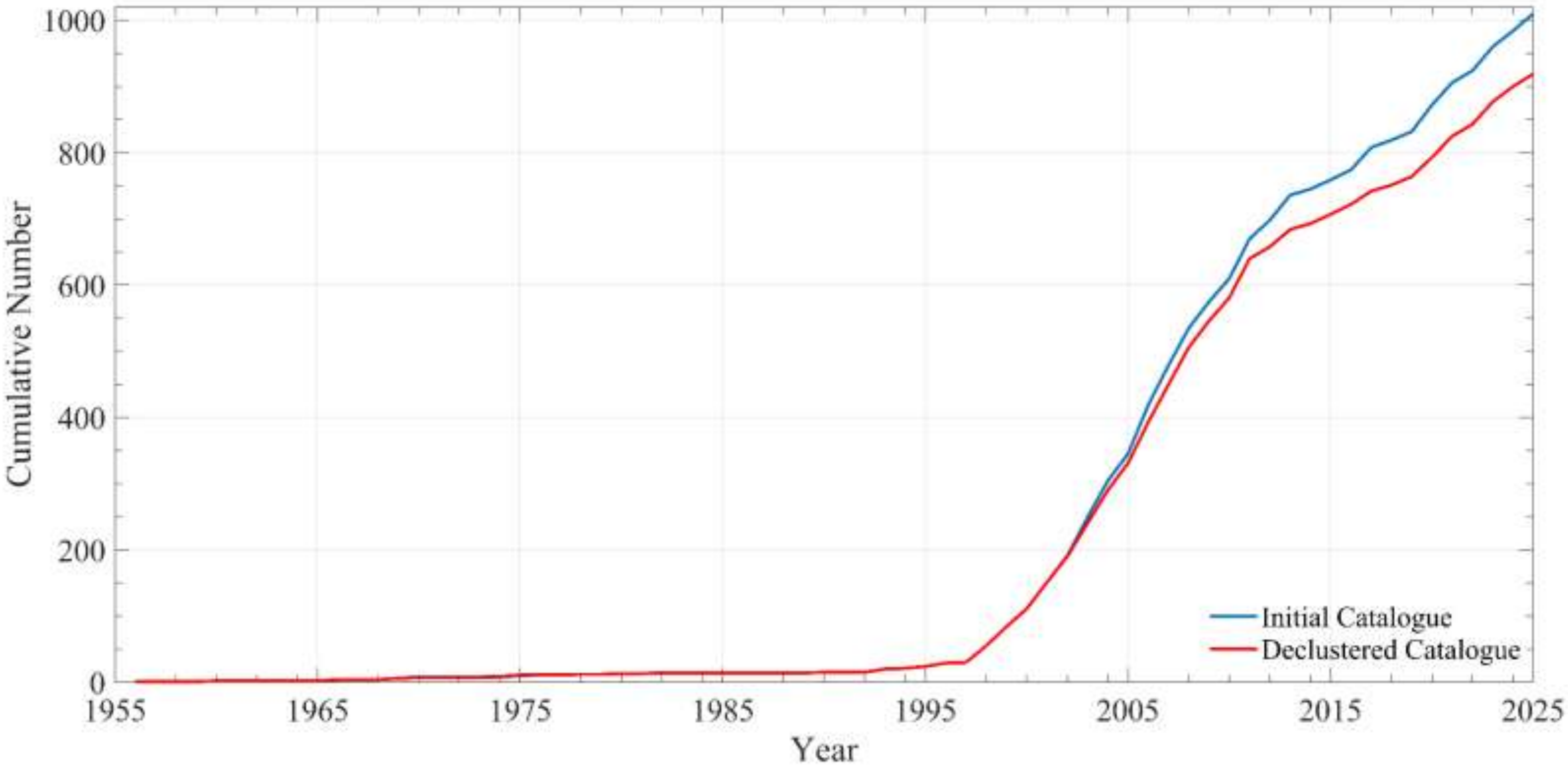

Figure 3: Declustering of the earthquake catalogue.

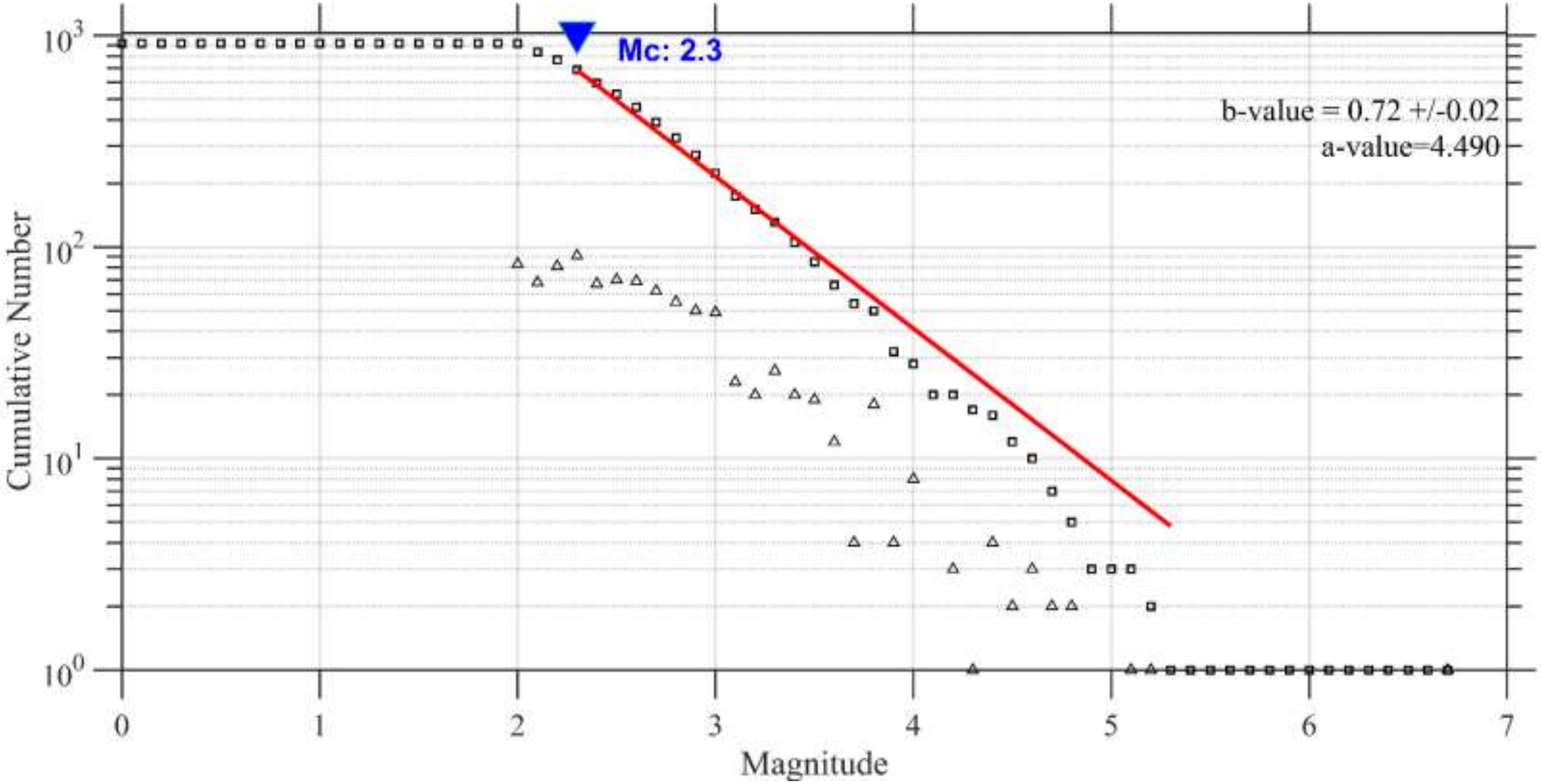

Figure 4: Frequency-magnitude distribution of the catalogue for the study period showing M_c; open squares indicate cumulative events and open triangles show non-cumulative events.

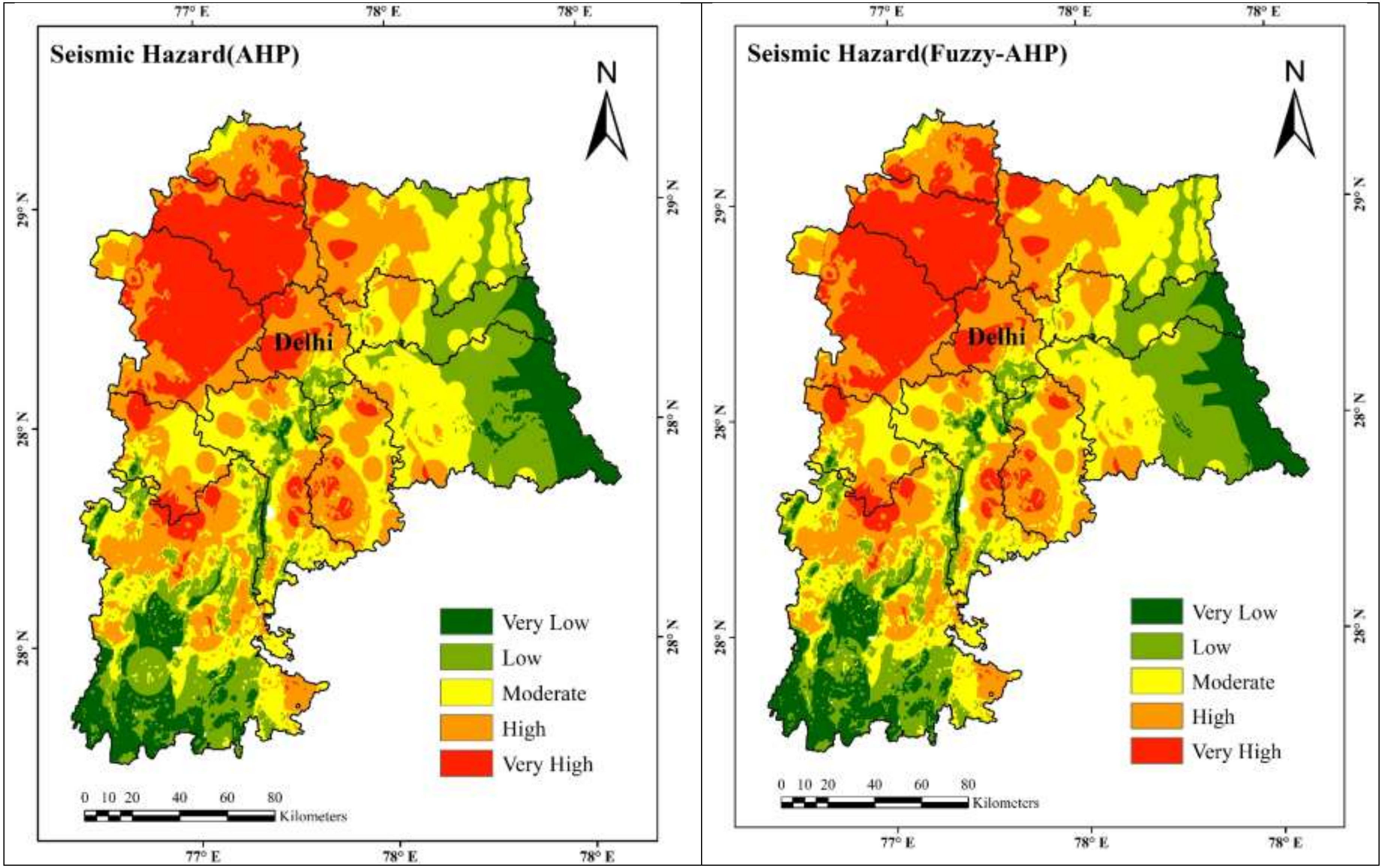
Seismic Hazard(AHP)
N
Delhi
Very Low
Low
Moderate
High
Very High
0 10 20 40 60 80
Kilometers
77° E
78° E
78° E
29° N
28° N
28° N
Seismic Hazard(Fuzzy-AHP)
N
Delhi
Very Low
Low
Moderate
High
Very High
0 10 20 40 60 80
Kilometers
77° E
78° E
78° E
29° N
28° N
28° N

Figure 5: Seismic hazard map of the study area using the AHP model and Fuzzy-AHP.

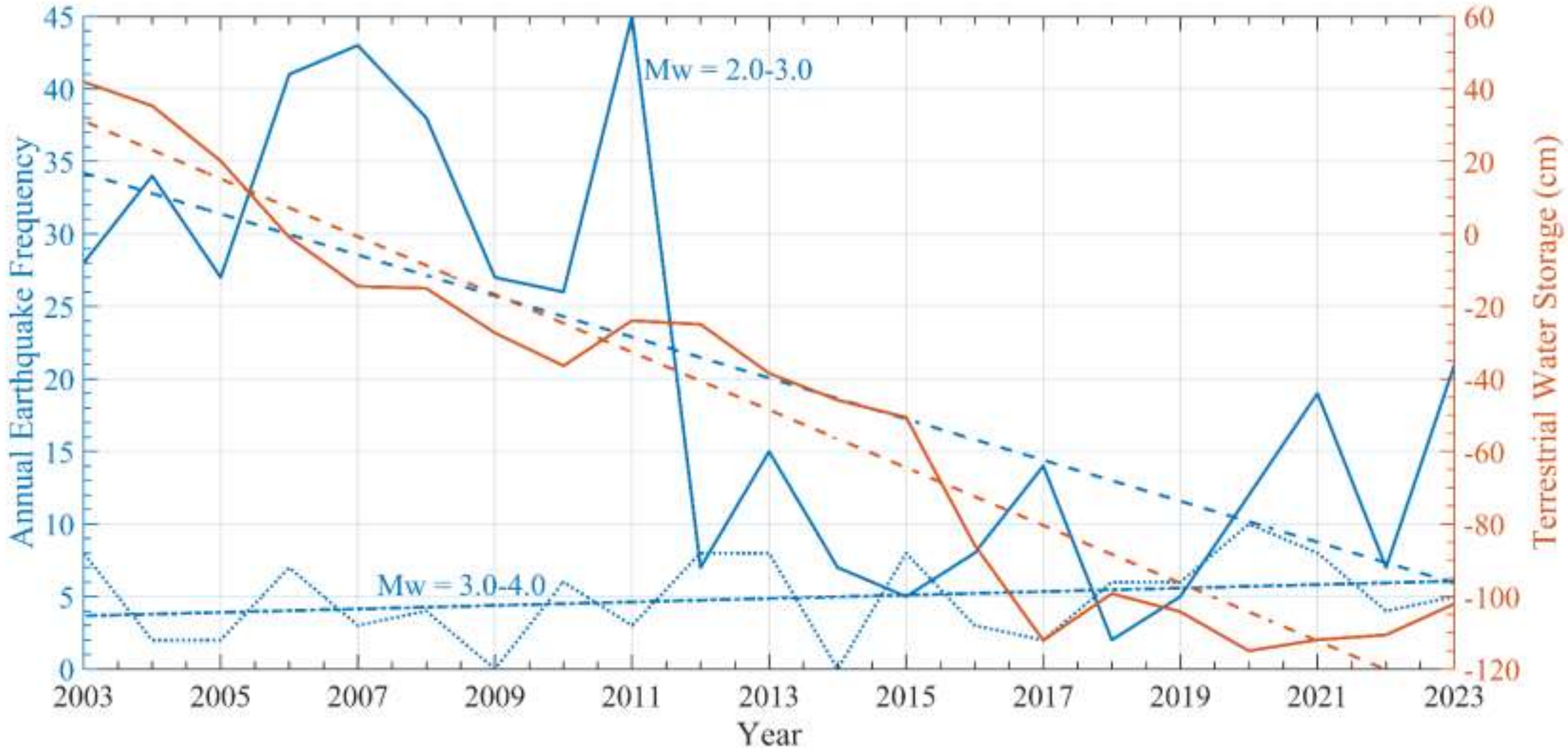

Figure 6: Graph showing the annual earthquake frequency (blue line) and terrestrial water storage (red line) during the period 2003-2023 for the Delhi-NCR. The dashed line shows the slope of the earthquake frequency and terrestrial water storage.

(a)

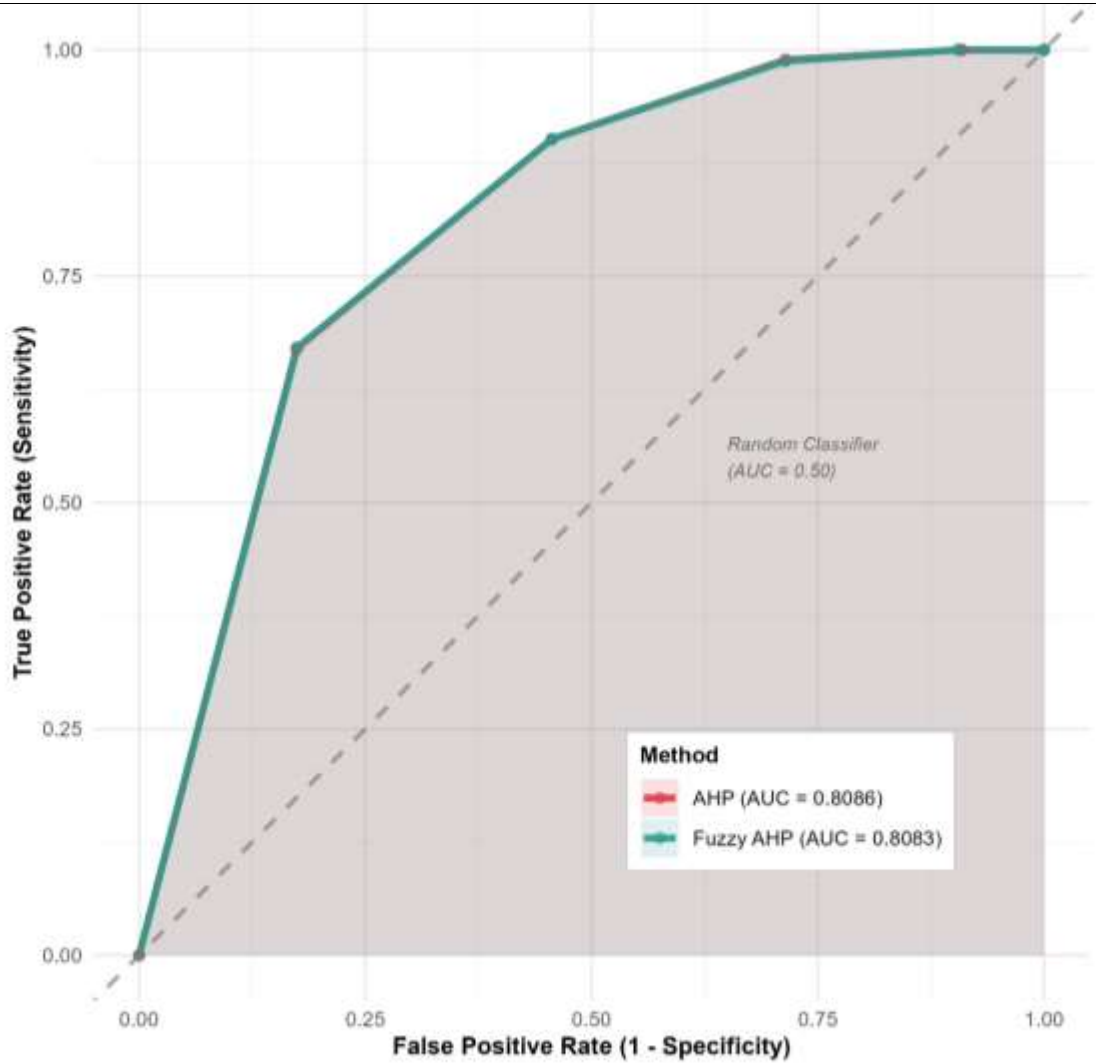

True Positive Rate (Sensitivity)
1.00
0.75
0.50
0.25
0.00
Random Classifier
(AUC = 0.50)
Method
AHP (AUC = 0.8086)
Fuzzy AHP (AUC = 0.8083)
0.00
0.25
0.50
0.75
1.00
False Positive Rate (1 - Specificity)

(b)

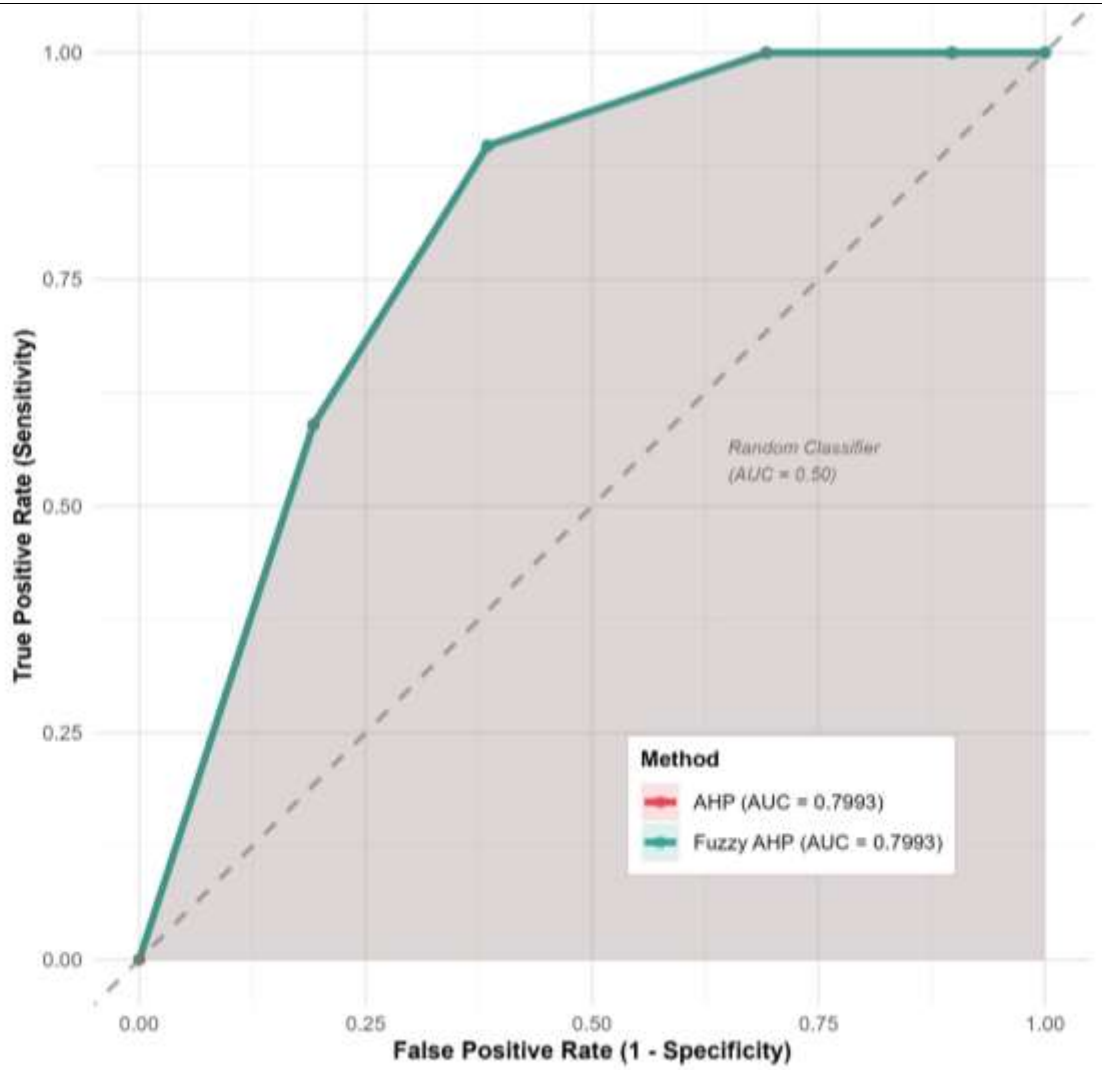
1.00
0.75
0.50
0.25
0.00
True Positive Rate (Sensitivity)
Random Classifier
(AUC = 0.50)
Method
AHP (AUC = 0.7993)
Fuzzy AHP (AUC = 0.7993)
0.00
0.25
0.50
0.75
1.00
False Positive Rate (1 - Specificity)

Figure 7: ROC curve showing the accuracy of seismic hazard in the study area using AHP and fuzzy-AHP using (a) the entire declustered dataset (1956-2025) and (b) 2024 and 2025 events. The dotted black line represents a random classifier

Table 1: Scale used for AHP (Saaty, 1980) and fuzzy AHP (Kannan et al., 2013) for pairwise comparison of each criterion

Relative Importance	Score	Triangular fuzzy scale
Equal	1	(1,1,1)
Moderate	3	(2,3,4)
Strong	5	(4,5,6)
Very Strong	7	(6,7,8)
Extreme	9	(9,9,9)
Intermediate Values	2, 4, 6, 8	(1,2,3), (3,4,5), (5,6,7), (7,8,9)
Values for reverse comparison	Reciprocals	Reciprocals

Table 2: Random Index (RI) values corresponding to various matrix sizes (n), as proposed by Saaty (1980) for a consistency check in AHP

n	1	2	3	4	5
RI	0.00	0.00	0.58	0.90	1.12
n	6	7	8	9	10
RI	1.24	1.32	1.41	1.45	1.49

Table 3: Seismic hazard parameters with their uncertainties for the study area

Seismic Zones	Number of Events (M_w ≥ 2.0)	M_c	M_{max} (Observed)	M_{max} (Kijko)	λ ± σ λ	β ± σβ	b value (Kijko 2004)	b value (Reyes and Wiemer, 2019)	a value
Zone 1	42	3.1	4.8	5.30±0.01	0.260±0.097	2.33±0.56	1.01± 0.24	0.97±0.34	4.106
Zone 2	27	2.8	3.6	4.10±0.31	0.502±0.188	3.45±0.05	1.50±0.02	1.55±0.42	5.445
Zone 3	66	2.7	6.7	7.20±0.01	0.428±0.133	2.16±0.34	0.94±0.15	0.84±0.23	3.732
Zone 4	138	2.1	5.2	5.70±0.36	2.050±0.545	1.43±0.09	0.62±0.04	0.61±0.05	3.364
Zone 5	118	2.0	4.8	5.30±0.51	1.789±0.477	1.79±0.12	0.78±0.05	0.74±0.07	3.562
Zone 6	82	2.2	3.8	4.30±0.10	1.359±0.374	1.66±0.12	0.72±0.05	0.73±0.06	3.484
Zone 7	85	2.2	4.0	4.50±0.14	2.570±0.710	1.62±0.12	0.70±0.05	0.71±0.06	3.414
Zone 8	298	2.3	5.1	5.60±0.22	3.878±1.004	1.73±0.08	0.75±0.03	0.73±0.04	4.012
Zone 9	63	2.7	4.5	5.00±0.01	0.998±0.311	3.22±0.45	1.40±0.19	1.28±0.26	4.915

Table 4: Weight calculation of seismic hazard-mapping parameters.

	1	2	3	4	5	6	7	8	9
1	1	2	2	3	3	4	4	5	6
2	0.5	1	2	2	3	3	4	4	5
3	0.5	0.5	1	2	2	3	3	4	4
4	0.33	0.5	0.5	1	2	2	3	3	4
5	0.33	0.33	0.5	0.5	1	2	2	3	3
6	0.25	0.33	0.33	0.5	0.5	1	2	2	3
7	0.25	0.25	0.33	0.33	0.5	0.5	1	2	3
8	0.2	0.25	0.25	0.33	0.33	0.5	0.5	1	2
9	0.17	0.2	0.25	0.25	0.33	0.33	0.33	0.5	1

	1	2	3	4	5	6	7	8	9
1	(1,1,1)	(1,2,3)	(1,2,3)	(2,3,4)	(2,3,4)	(3,4,5)	(3,4,5)	(4,5,6)	(5,6,7)
2	(1/3,1/2,1)	(1,1,1)	(1,2,3)	(1,2,3)	(2,3,4)	(2,3,4)	(3,4,5)	(3,4,5)	(4,5,6)
3	(1/3,1/2,1)	(1/3,1/2,1)	(1,1,1)	(1,2,3)	(1,2,3)	(2,3,4)	(2,3,4)	(3,4,5)	(3,4,5)
4	(1/4,1/3,1/2)	(1/3,1/2,1)	(1/3,1/2,1)	(1,1,1)	(1,2,3)	(1,2,3)	(2,3,4)	(2,3,4)	(3,4,5)
5	(1/4,1/3,1/2)	(1/4,1/3,1/2)	(1/3,1/2,1)	(1/3,1/2,1)	(1,1,1)	(1,2,3)	(1,2,3)	(2,3,4)	(2,3,4)
6	(1/5,1/4,1/3)	(1/4,1/3,1/2)	(1/4,1/3,1/2)	(1/3,1/2,1)	(1/3,1/2,1)	(1,1,1)	(1,2,3)	(1,2,3)	(2,3,4)
7	(1/5,1/4,1/3)	(1/5,1/4,1/3)	(1/4,1/3,1/2)	(1/4,1/3,1/2)	(1/3,1/2,1)	(1/3,1/2,1)	(1,1,1)	(1,2,3)	(2,3,4)
8	(1/6,1/5,1/4)	(1/5,1/4,1/3)	(1/5,1/4,1/3)	(1/4,1/3,1/2)	(1/4,1/3,1/2)	(1/3,1/2,1)	(1/3,1/2,1)	(1,1,1)	(1,2,3)
9	(1/7,1/6,1/5)	(1/6,1/5,1/4)	(1/5,1/4,1/3)	(1/5,1/4,1/3)	(1/4,1/3,1/2)	(1/4,1/3,1/2)	(1/4,1/3,1/2)	(1/3,1/2,1)	(1,1,1)

Sl. No.	Selected Layers	AHP Weight	Fuzzy AHP Weight
1	Distance from Faults (km)	25.80%	24.90%
2	Distance from Epicentres (km)	19.50%	19.40%
3	Seismic Density (Earthquakes/km^2)	15.10%	15.10%
4	V_{s30} (m/sec)	11.60%	12.00%
5	Peak Ground Acceleration (cm/sec^2)	8.90%	9.10%
6	Amplification Factor	6.80%	6.90%
7	Sediment Thickness (m)	5.50%	5.40%
8	Lithology	3.90%	4.00%
9	Elevation (m)	2.90%	3.10%
Principal Eigen Value		9.311	9.719
Consistency Ratio (CR)		0.027	0.062

Table 5: Seismic hazard exposure of area and population in Delhi–NCR

Seismic Hazard	Classes	Area (%)	Population (%)
AHP	Very low	9.66	4.55
	Low	18.02	15.13
	Moderate	26.99	26.26
	High	27.39	39.15
	Very high	17.95	14.91
Fuzzy AHP	Very low	9.84	4.51
	Low	17.94	15.21
	Moderate	26.72	25.96
	High	27.49	39.39
	Very high	18.01	14.93

Table 6: Comparison of PGA values reported in various studies.

Studies	**Return periods (years)**	**PGA (g)**
Sharma et al. (2003)	475	0.00-0.34
Iyenger and Ghosh (2004)	2475	0.00-0.23
Nath and Thingbaijam (2012)	475	0.00-0.24
Sitharam and Kolathayar (2013)	475	0.00-0.16
	2475	0.00-0.43
Sitharam et al. (2015)	475	0.00-0.27
	2475	0.00-0.51
Sreejaya et al. (2022)	73	0.00-0.05
	475	0.00-0.18
	2475	0.00-0.41
Kumar et al. (2024)	73	0.01-0.10
	475	0.03-0.26
	2475	0.05-0.48

Table 7: Normalised AHP comparison matrix along with final preferences and all possible $\delta_{k,i,j}$ Values

	1	**2**	**3**	**4**	**5**	**6**	**7**	**8**	**9**	**Pi**
1	0.073	0.073	0.042	0.035	0.021	0.017	0.011	0.008	0.006	0.286
2	0.037	0.036	0.042	0.023	0.021	0.012	0.011	0.007	0.005	0.194
3	0.037	0.018	0.021	0.023	0.014	0.012	0.008	0.007	0.004	0.144
4	0.024	0.018	0.011	0.012	0.014	0.008	0.008	0.005	0.004	0.104
5	0.024	0.012	0.011	0.006	0.007	0.008	0.006	0.005	0.003	0.081
6	0.018	0.012	0.007	0.006	0.003	0.004	0.006	0.003	0.003	0.062
7	0.018	0.009	0.007	0.004	0.003	0.002	0.003	0.003	0.003	0.053
8	0.015	0.009	0.005	0.004	0.002	0.002	0.001	0.002	0.002	0.042
9	0.012	0.007	0.005	0.003	0.002	0.001	0.001	0.001	0.001	0.034

Pair of Alternatives	**1**	**2**	**3**	**4**	**5**	**6**	**7**	**8**	**9**
A1-A2	N/F	N/F	N/F	N/F	N/F	N/F	N/F	N/F	N/F
A1-A3	N/F	N/F	N/F	N/F	N/F	N/F	N/F	N/F	N/F
A1-A4	N/F	N/F	N/F	N/F	N/F	N/F	N/F	N/F	N/F
A1-A5	N/F	N/F	N/F	N/F	N/F	N/F	N/F	N/F	N/F
A1-A6	N/F	N/F	N/F	N/F	N/F	N/F	N/F	N/F	N/F
A1-A7	N/F	N/F	N/F	N/F	N/F	N/F	N/F	N/F	N/F
A1-A8	N/F	N/F	N/F	N/F	N/F	N/F	N/F	N/F	N/F
A1-A9	N/F	N/F	N/F	N/F	N/F	N/F	N/F	N/F	N/F
A2-A3	N/F	N/F	N/F	N/F	N/F	N/F	N/F	N/F	N/F
A2-A4	N/F	N/F	N/F	N/F	N/F	N/F	N/F	N/F	N/F
A2-A5	N/F	N/F	N/F	N/F	N/F	N/F	N/F	N/F	N/F
A2-A6	N/F	N/F	N/F	N/F	N/F	N/F	N/F	N/F	N/F
A2-A7	N/F	N/F	N/F	N/F	N/F	N/F	N/F	N/F	N/F
A2-A8	N/F	N/F	N/F	N/F	N/F	N/F	N/F	N/F	N/F
A2-A9	N/F	N/F	N/F	N/F	N/F	N/F	N/F	N/F	N/F
A3-A4	N/F	N/F	N/F	N/F	N/F	N/F	N/F	N/F	N/F
A3-A5	N/F	N/F	N/F	N/F	N/F	N/F	N/F	N/F	N/F
A3-A6	N/F	N/F	N/F	N/F	N/F	N/F	N/F	N/F	N/F
A3-A7	N/F	N/F	N/F	N/F	N/F	N/F	N/F	N/F	N/F
A3-A8	N/F	N/F	N/F	N/F	N/F	N/F	N/F	N/F	N/F
A3-A9	N/F	N/F	N/F	N/F	N/F	N/F	N/F	N/F	N/F
A4-A5	N/F	N/F	N/F	N/F	N/F	N/F	N/F	N/F	N/F
A4-A6	N/F	N/F	N/F	N/F	N/F	N/F	N/F	N/F	N/F
A4-A7	N/F	N/F	N/F	N/F	N/F	N/F	N/F	N/F	N/F
A4-A8	N/F	N/F	N/F	N/F	N/F	N/F	N/F	N/F	N/F
A4-A9	N/F	N/F	N/F	N/F	N/F	N/F	N/F	N/F	N/F

A5-A6	N/F	N/F	N/F	N/F	N/F	N/F	N/F	N/F	N/F
A5-A7	N/F	N/F	N/F	N/F	N/F	N/F	N/F	N/F	N/F
A5-A8	N/F	N/F	N/F	N/F	N/F	N/F	N/F	N/F	N/F
A5-A9	N/F	N/F	N/F	N/F	N/F	N/F	N/F	N/F	N/F
A6-A7	N/F	N/F	N/F	N/F	N/F	N/F	N/F	N/F	N/F
A6-A8	N/F	N/F	N/F	N/F	N/F	N/F	N/F	N/F	N/F
A6-A9	N/F	N/F	N/F	N/F	N/F	N/F	N/F	N/F	N/F
A7-A8	N/F	N/F	N/F	N/F	N/F	N/F	N/F	N/F	N/F
A7-A9	N/F	N/F	N/F	N/F	N/F	N/F	N/F	N/F	N/F
A8-A9	N/F	N/F	N/F	N/F	N/F	N/F	N/F	N/F	N/F

A1: Distance from Faults; *A2*: Distance from Epicentres; *A3*: Seismic Density; *A4*: V_{s30}; *A5*: Peak Ground Acceleration; *A6*: Amplification Factor; *A7*: Sediment Thickness; *A8*: Lithology; *A9*: Elevation

N/F stands for non-feasible.

Table 8: Normalised Fuzzy-AHP comparison matrix along with final preferences and all possible $\delta_{k,i,j}$ Values

	1	**2**	**3**	**4**	**5**	**6**	**7**	**8**	**9**	**Pi**
1	(0.348, 0.283, 0.196)	(0.268, 0.373, 0.379)	(0.219, 0.279, 0.281)	(0.314, 0.302, 0.279)	(0.245, 0.237, 0.222)	(0.275, 0.245, 0.222)	(0.221, 0.202, 0.189)	(0.231, 0.204, 0.188)	(0.217, 0.194, 0.180)	(0.140, 0.289, 0.512)
2	(0.116, 0.142, 0.196)	(0.268, 0.186, 0.126)	(0.219, 0.279, 0.281)	(0.157, 0.202, 0.209)	(0.245, 0.237, 0.222)	(0.183, 0.184, 0.178)	(0.221, 0.202, 0.189)	(0.231, 0.204, 0.188)	(0.174, 0.161, 0.154)	(0.097, 0.197, 0.391)
3	(0.116, 0.142, 0.196)	(0.089, 0.093, 0.126)	(0.219, 0.140, 0.094)	(0.157, 0.202, 0.209)	(0.123, 0.158, 0.167)	(0.183, 0.184, 0.178)	(0.147, 0.151, 0.151)	(0.173, 0.163, 0.156)	(0.130, 0.129, 0.128)	(0.070, 0.127, 0.225)
4	(0.087, 0.094, 0.098)	(0.089, 0.093, 0.126)	(0.073, 0.070, 0.094)	(0.157, 0.101, 0.070)	(0.123, 0.158, 0.167)	(0.092, 0.123, 0.133)	(0.147, 0.151, 0.151)	(0.115, 0.122, 0.125)	(0.130, 0.129, 0.128)	(0.062, 0.104, 0.174)
5	(0.087, 0.094, 0.098)	(0.067, 0.062, 0.063)	(0.073, 0.070, 0.094)	(0.052, 0.050, 0.070)	(0.123, 0.079, 0.056)	(0.092, 0.123, 0.133)	(0.074, 0.101, 0.113)	(0.115, 0.122, 0.125)	(0.087, 0.097, 0.103)	(0.042, 0.073, 0.120)
6	(0.070, 0.071, 0.065)	(0.067, 0.062, 0.063)	(0.055, 0.047, 0.047)	(0.052, 0.050, 0.070)	(0.041, 0.040, 0.056)	(0.092, 0.123, 0.133)	(0.074, 0.101, 0.113)	(0.058, 0.082, 0.094)	(0.087, 0.097, 0.103)	(0.029, 0.054, 0.086)
7	(0.070, 0.071, 0.065)	(0.054, 0.047, 0.042)	(0.055, 0.047, 0.047)	(0.052, 0.050, 0.070)	(0.041, 0.040, 0.056)	(0.031, 0.031, 0.044)	(0.074, 0.050, 0.038)	(0.058, 0.082, 0.094)	(0.087, 0.097, 0.103)	(0.026, 0.048, 0.078)
8	(0.058, 0.057, 0.049)	(0.054, 0.047, 0.042)	(0.044, 0.035, 0.031)	(0.039, 0.034, 0.035)	(0.031, 0.026, 0.028)	(0.031, 0.031, 0.044)	(0.025, 0.025, 0.038)	(0.058, 0.041, 0.031)	(0.044, 0.065, 0.077)	(0.017, 0.033, 0.055)
9	(0.050, 0.047, 0.039)	(0.045, 0.037, 0.032)	(0.044, 0.035, 0.031)	(0.031, 0.025, 0.023)	(0.031, 0.026, 0.028)	(0.023, 0.020, 0.022)	(0.025, 0.025, 0.038)	(0.019, 0.020, 0.031)	(0.044, 0.032, 0.026)	(0.012, 0.022, 0.034)

Pair of Alternatives	1	2	3	4	5	6	7	8	9
A1-A2	N/F	N/F	N/F	N/F	N/F	N/F	N/F	N/F	N/F
A1-A3	N/F	N/F	N/F	N/F	N/F	N/F	N/F	N/F	N/F
A1-A4	N/F	N/F	N/F	N/F	N/F	N/F	N/F	N/F	N/F
A1-A5	N/F	N/F	N/F	N/F	N/F	N/F	N/F	N/F	N/F
A1-A6	N/F	N/F	N/F	N/F	N/F	N/F	N/F	N/F	N/F
A1-A7	N/F	N/F	N/F	N/F	N/F	N/F	N/F	N/F	N/F
A1-A8	N/F	N/F	N/F	N/F	N/F	N/F	N/F	N/F	N/F
A1-A9	N/F	N/F	N/F	N/F	N/F	N/F	N/F	N/F	N/F
A2-A3	N/F	N/F	N/F	N/F	N/F	N/F	N/F	N/F	N/F
A2-A4	N/F	N/F	N/F	N/F	N/F	N/F	N/F	N/F	N/F
A2-A5	N/F	N/F	N/F	N/F	N/F	N/F	N/F	N/F	N/F
A2-A6	N/F	N/F	N/F	N/F	N/F	N/F	N/F	N/F	N/F
A2-A7	N/F	N/F	N/F	N/F	N/F	N/F	N/F	N/F	N/F
A2-A8	N/F	N/F	N/F	N/F	N/F	N/F	N/F	N/F	N/F
A2-A9	N/F	N/F	N/F	N/F	N/F	N/F	N/F	N/F	N/F
A3-A4	N/F	N/F	N/F	N/F	N/F	N/F	N/F	N/F	N/F
A3-A5	N/F	N/F	N/F	N/F	N/F	N/F	N/F	N/F	N/F
A3-A6	N/F	N/F	N/F	N/F	N/F	N/F	N/F	N/F	N/F
A3-A7	N/F	N/F	N/F	N/F	N/F	N/F	N/F	N/F	N/F
A3-A8	N/F	N/F	N/F	N/F	N/F	N/F	N/F	N/F	N/F
A3-A9	N/F	N/F	N/F	N/F	N/F	N/F	N/F	N/F	N/F
A4-A5	N/F	N/F	N/F	N/F	N/F	N/F	N/F	N/F	N/F
A4-A6	N/F	N/F	N/F	N/F	N/F	N/F	N/F	N/F	N/F
A4-A7	N/F	N/F	N/F	N/F	N/F	N/F	N/F	N/F	N/F
A4-A8	N/F	N/F	N/F	N/F	N/F	N/F	N/F	N/F	N/F
A4-A9	N/F	N/F	N/F	N/F	N/F	N/F	N/F	N/F	N/F
A5-A6	N/F	N/F	N/F	N/F	N/F	N/F	N/F	N/F	N/F
A5-A7	N/F	N/F	N/F	N/F	N/F	N/F	N/F	N/F	N/F
A5-A8	N/F	N/F	N/F	N/F	N/F	N/F	N/F	N/F	N/F
A5-A9	N/F	N/F	N/F	N/F	N/F	N/F	N/F	N/F	N/F
A6-A7	N/F	N/F	N/F	N/F	N/F	N/F	N/F	N/F	N/F
A6-A8	N/F	N/F	N/F	N/F	N/F	N/F	N/F	N/F	N/F
A6-A9	N/F	N/F	N/F	N/F	N/F	N/F	N/F	N/F	N/F
A7-A8	N/F	N/F	N/F	N/F	N/F	N/F	N/F	N/F	N/F
A7-A9	N/F	N/F	N/F	N/F	N/F	N/F	N/F	N/F	N/F
A8-A9	N/F	N/F	N/F	N/F	N/F	N/F	N/F	N/F	N/F

N/F stands for non-feasible.